THE JOURNAL OF PHYSICAL CHEMISTRY B

Article

pubs.acs.org/JPCB

Complementary Fluorescence and Phosphorescence Study of the Interaction of Brompheniramine with Human Serum Albumin

Silvia Tardioli,† Ivonne Lammers,† Jan-Hein Hooijschuur, Freek Ariese, Gert van der Zwan,* and Cees Gooijer

Department of Biomolecular Analysis and Spectroscopy, LaserLaB, VU University Amsterdam, De Boelelaan 1083, 1081 HV Amsterdam, The Netherlands

ABSTRACT: Binding of the antihistamine drug brompheniramine (BPA) to human serum albumin (HSA) is studied by measuring quenching of the fluorescence and room temperature phosphorescence (RTP) of tryptophan. The modified Stern−Volmer equation was used to derive association constants and accessible fractions from the steady-state fluorescence data. Decay associated spectra (DAS) revealed three tryptophan fluorescence lifetimes, indicating the presence of three HSA conformations. BPA causes mainly static quenching of the long-living, solvent-exposed conformer. RTP spectra and lifetimes, recorded under deoxygenated conditions in the presence of 0.2 M KI, provided additional kinetic information about the HSA−BPA interactions. Fluorescence DAS that were also recorded in the presence of 0.2 M KI revealed that the solvent-exposed conformer is the major contributor to the RTP signal. The phosphorescence quenching is mostly dynamic at pH 7 and mostly static at pH 9, presumably related to the protonation state of the alkylamino chain of BPA. This provides direct insight into the binding mode of the antihistamine drug, as well as kinetic information at both the nanosecond and the millisecond time scales.

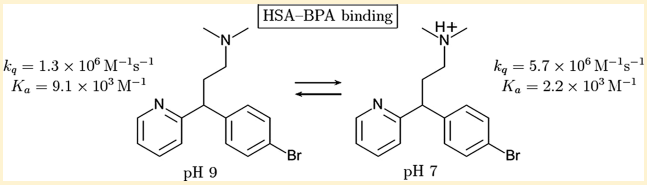

INTRODUCTION

Binding of drugs to the transport protein human serum albumin (HSA) has been the subject of a large number of investigations. A wide variety of techniques has been applied for this purpose, based on separation methods on the one hand and spectroscopic methods on the other, with focus on binding constants.[1−7] However, it is still a challenge to interpret these binding constants since various binding sites of HSA are available.[8] For pharmacokinetic modeling, the results of such studies should preferably be combined with information about the dynamics.

HSA contains only a single tryptophan, and this amino acid is situated near a primary binding site; as a result, in principle fluorescence spectroscopy at selective wavelengths can provide direct information about the effects of ligand binding if it influences the properties of that tryptophan. Unfortunately, as is well-known from literature,[9] even proteins with a single tryptophan residue often still show more than a single fluorescence lifetime, which can be attributed to the existence of multiple protein conformations. This is also the case for HSA. Since nearby amino acid residues can act as quenchers of tryptophan fluorescence, even slightly different protein conformations can result in different decay times. The longest lifetime (as long as 7 ns) of single-tryptophan proteins is usually observed at the red side of the emission spectrum and is attributed to water-exposed tryptophan residues. Buried tryptophans often show shorter lifetimes as a result of the above-mentioned quenching effects from certain amino acids.[9]

For (static) fluorescence quenching in proteins with more than one tryptophan, the Stern−Volmer plot will be nonlinear when the individual fluorophores are not equally accessible to the quencher Q.[10,11] Instead, a modified Stern−Volmer equation has to be used, given by

$$\frac{F_0}{\Delta F} = \frac{1}{f_a K_a [Q]} + \frac{1}{f_a} \quad (1)$$

where $\Delta F = F_0 - F$ in which F_0 and F represent the fluorescence intensities of the protein in the absence and in the presence of quencher, respectively, and $[Q]$ is the quencher concentration.[9] From a plot of $F_0/\Delta F$ vs $[Q]^{-1}$, one can obtain the values of the fractional accessible tryptophans f_a and the quencher association constant K_a. The question needs to be addressed whether in the case of HSA, which only contains a single tryptophan but is present in more conformations, differences in accessibility also play a role. Static fluorescence quenching experiments of HSA with the antihistamine compound chlorpheniramine seem to suggest this.[12] In the present paper, we investigate fluorescence quenching phenomena of a similar compound, that is, the antihistamine brompheniramine (BPA, see Figure 1), not only by steady-state fluorescence but also in the time-resolved fluorescence mode, by recording decay associated spectra (DAS) to study these phenomena in more detail.

The tryptophan moiety is not only fluorescent but can also emit phosphorescence at room temperature (RTP), as is already known for proteins since 1974.[13] RTP of HSA under

Received: January 3, 2012
Revised: May 18, 2012
Published: May 21, 2012

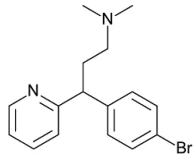

Figure 1. Molecular structure of BPA; the protonated form is dominant at neutral pH. A racemic mixture was used for this study.

liquid conditions is not easily detected, but Wei and co-workers[14] showed that intense phosphorescence spectra can be obtained if the samples are deoxygenated and KI is added as heavy atom reagent. Phosphorescence can provide valuable information about protein structure and dynamics in the micro- to milliseconds regime, in contrast to fluorescence phenomena, which take place on a nanosecond time scale. Proteins with a single tryptophan residue may show more than a single phosphorescence lifetime, indicating the presence of multiple conformations that are stable at the phosphorescence time scale.[15,16] In this work, in addition to the fluorescence data, complementary phosphorescence information about HSA–BPA binding will be obtained in the spectral as well as in the time domain.

As far as we know, for the interaction of BPA and HSA only the overall binding constant has been determined. Martinez-Gomez and co-workers[4] determined the fraction of unbound drug at various HSA levels in a capillary electrophoresis setup at pH 7.4 and derived an association constant of $(1.8 \pm 0.3) \times 10^3$ M^{-1}. For those experiments, the authors had to assume that there is only a single active binding site. In this paper, we aim to gain insight into complex quenching phenomena, the binding mode, and the pH dependence of drug binding, as well as binding kinetics.

EXPERIMENTAL SECTION

Chemicals. Fatty acid free albumin from human serum (≥96%), L-tryptophan, (±)-brompheniramine maleate salt, boric acid, potassium iodide, and sodium sulfite were purchased from Sigma-Aldrich (St. Louis, MO, USA), and sodium hydroxide was from Fluka (Buchs, Switzerland). Potassium dihydrogen phosphate and potassium monohydrogen phosphate were obtained from J.T. Baker (Deventer, The Netherlands). All chemicals were used as received. Water was purified with a Milli-Q system from Millipore (Bedford, MA, USA).

Fluorescence. Fluorescence emission spectra were recorded at room temperature on a LS50-B spectrometer, using a square quartz cuvette of 10 mm path length. All measurements were performed at an excitation wavelength of 295 nm and spectral band widths of 10 nm. Static fluorescence spectra of HSA and BPA mixtures were determined in 10 mM phosphate buffer (pH 7.2) or 10 mM borate buffer (pH 9.0), at a fixed protein concentration of 4 μM and varying BPA concentrations: 0.10, 0.27, 0.61, and 1.63 mM. The emission at 350 nm was used to construct Stern–Volmer plots.

Time correlated single photon counting (TCSPC) was used to determine fluorescence intensity decays. The excitation source was a Ti:Sapph laser (Coherent, Mira 900, Santa Clara, CA, USA) with a pulse width of 3 ps. The output of the laser was frequency tripled to get the excitation wavelength of 295 nm. A multichannel-plate photomultiplier (Hamamatsu, R3809U-50, Japan) collected the fluorescence emission, and data were recorded through a SPC-630 module (Becker & Hickl GmbH, Berlin, Germany) with a time resolution of 15 ps. Fluorescence decay curves were analyzed using a global fitting procedure based on the Levenberg–Marquardt algorithm. The instrument response function (determined by collecting scattered light from a suspension of silica particles) was used for deconvolution of the recorded decays and for determination of lifetimes and wavelength-dependent amplitudes. Each intensity curve was fitted with a multiexponential decay, and the goodness of fit was assessed on the basis of χ^2 and the distribution of residuals.

The decay-associated spectra were constructed by distributing the total intensity per decay curve over the lifetimes that make up the total intensity according to their amplitudes obtained by the above fit procedure. The relative fluorescence intensity $I_j(\lambda)$ of lifetime component τ_j at wavelength λ with amplitude $A_j(\lambda)$ can be expressed by the following equation:

$$I_j(\lambda) = \frac{A_j(\lambda)\tau_j}{\sum_i A_i(\lambda)\tau_i} \quad (2)$$

The sum in the denominator of this expression is equal to the steady-state emission spectrum.

All experiments were repeated five times ($n = 5$), from which the standard deviations of the measurements were calculated, given as error bars in Figures 2 and 3.

Phosphorescence. A Cary Eclipse luminescence spectrometer (Varian, Melbourne, Australia) was used for recording the HSA phosphorescence. For enhancing the phosphorescence emission, 0.2 M KI was added. Chemical deoxygenation was achieved by adding 2 mM Na_2SO_3 to the samples just before capping the 10 mm square quartz cuvettes. The temperature was kept at 20 °C using the single-cell Peltier cooler of the spectrometer. The phosphorescence emission spectra were recorded with an excitation wavelength of 290 nm, spectral band widths of 10 nm, a delay time of 0.1 ms, and a total gate time of 5 ms. The intensities were corrected for the signal loss during the delay time by multiplication with a correction factor depending on the phosphorescence lifetimes. Time-resolved phosphorescence decay curves for the lifetime measurements were obtained with an excitation wavelength of 290 nm, an emission wavelength of 443 nm, an initial delay of 50 μs, a gate width of 50 μs, and a total decay time of 15 ms. Origin 8.0 was used to fit the phosphorescence decay curves with a biexponential decay function, and the goodness of the fit was assessed on the basis of χ^2 and the distribution of residuals.

RESULTS AND DISCUSSION

Fluorescence. In this subsection on HSA tryptophan fluorescence, we will first present static and time-resolved fluorescence data on the quenching of 4 μM HSA by various concentrations (0–1.63 mM) of BPA. Excitation was at 295 nm, which is selective for tryptophan; other amino acid residues and BPA are not excited at that wavelength. Furthermore, the effect of adding KI was investigated in order to be able to couple the fluorescence with the phosphorescence results. To obtain more insight into the mechanism of fluorescence quenching, the experiments were carried out at pH 7.2 and at pH 9.0. Because of its alkylamine tail, BPA has a pK_a of 9.1,[17] which implies that at neutral pH the fraction of unprotonated BPA is negligible, whereas at pH 9.0 it is close to 50%. Binding to HSA can be influenced by the charge of the BPA tail, and therefore the equilibrium constant is expected to be pH dependent. Measurements at higher pH with fully deproto-

dx.doi.org/10.1021/jp300055c | J. Phys. Chem. B 2012, 116, 7033–7039

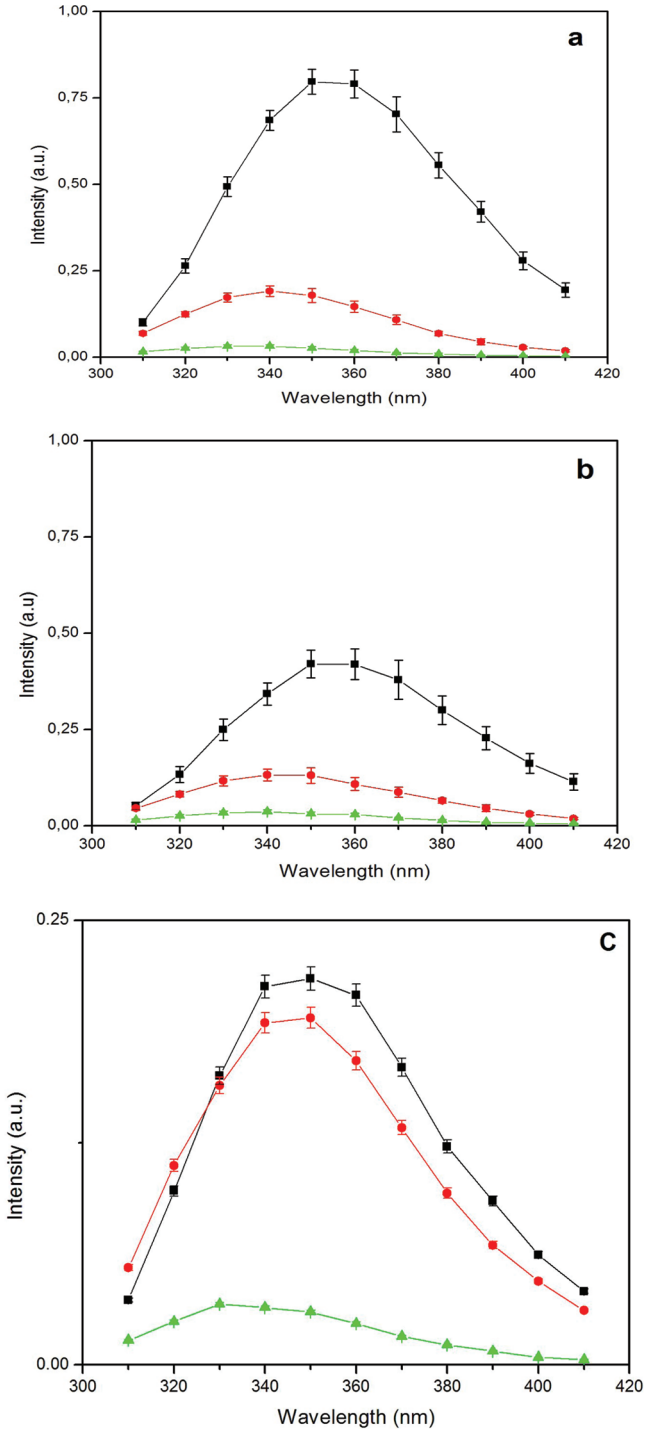

Figure 2. Decay associated fluorescence spectra of 4 μM HSA at pH 7.2. Frame (a): in the absence of BPA, ■ 7.2 ns, ● 2.6 ns, and ▲ 0.4 ns. Frame (b): in the presence of 1.6 mM BPA, ■ 6.9 ns, ● 2.6 ns, and ▲ 0.4 ns. Frame (c): in the presence of 0.2 M KI, ■ 4.6 ns, ● 1.8 ns, and ▲ 0.3 ns. The total intensity of graph a is normalized to 1; those of graphs b and c are on the same scale.

nated BPA could not be carried out because of protein denaturation under those conditions.

When plotting the steady-state quenching data using the regular Stern–Volmer equation, no linear relationship was obtained. Such behavior may be caused by differences in accessibility of the tryptophan. Indeed, at both pH values tested a modified Stern–Volmer equation resulted in a linear plot

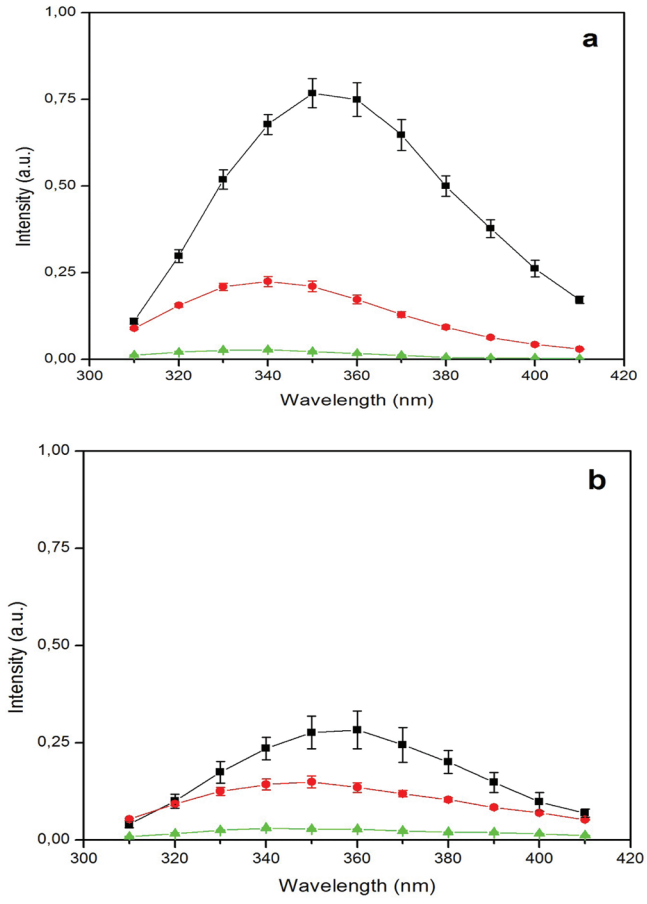

Figure 3. Decay associated fluorescence spectra of HSA 4 μM at pH 9.0. Frame (a): in absence of BPA, ■ 6.7 ns, ● 2.6 ns, and ▲ 0.4 ns. Frame (b): in presence of 1.6 mM BPA, ■ 5.8 ns, ● 2.6 ns, and ▲ 0.4 ns. The total intensity of graph a is normalized to 1; that of graph b is on the same scale.

(data not shown). The results of steady state fluorescence experiments did indeed show a strong pH dependence: at pH 7.2 the equilibrium binding constant was determined to be (2.2 ± 0.3) × 10^3 M^{-1} with f_a = 0.50 ± 0.03, but at pH 9.0 it was substantially higher: (9.1 ± 2.2) × 10^3 M^{-1} with f_a = 0.71 ± 0.03. The fact that the protonated ligand has a lower association constant may indicate a nonpolar binding mechanism.

In order to study these phenomena in more detail, time-resolved fluorescence experiments were performed. The DAS obtained for a pure HSA solution (no ligand) and in the presence of 1.63 mM BPA are shown in Figure 2 for pH 7.2 and in Figure 3 for pH 9.0. Without quencher at pH 7.2, three fluorescence lifetimes are obtained: 7.2, 2.6, and 0.4 ns. Upon increasing the pH to 9.0, these lifetimes hardly change: 6.7, 2.6, and 0.4 ns. The DAS corresponding to these three lifetimes (Figures 2a and 3a) are distinctly different: the maximum wavelength of the 7.2/6.7 ns fluorescence is at about 355 nm, some 15 nm red-shifted in comparison with that of the shorter-living species. These results are in accordance with other single-tryptophan proteins as discussed by Lakowicz.[9] In the following, these species will be referred to as conformers I, II, and III. The longer living component (conformer I) is found at longer emission wavelengths, indicating that it is exposed to a more polar environment, possibly water, whereas tryptophan residues buried inside the protein matrix (conformers II and III) have shorter lifetimes and emit at shorter wavelengths.

dx.doi.org/10.1021/jp300055c | J. Phys. Chem. B 2012, 116, 7033–7039

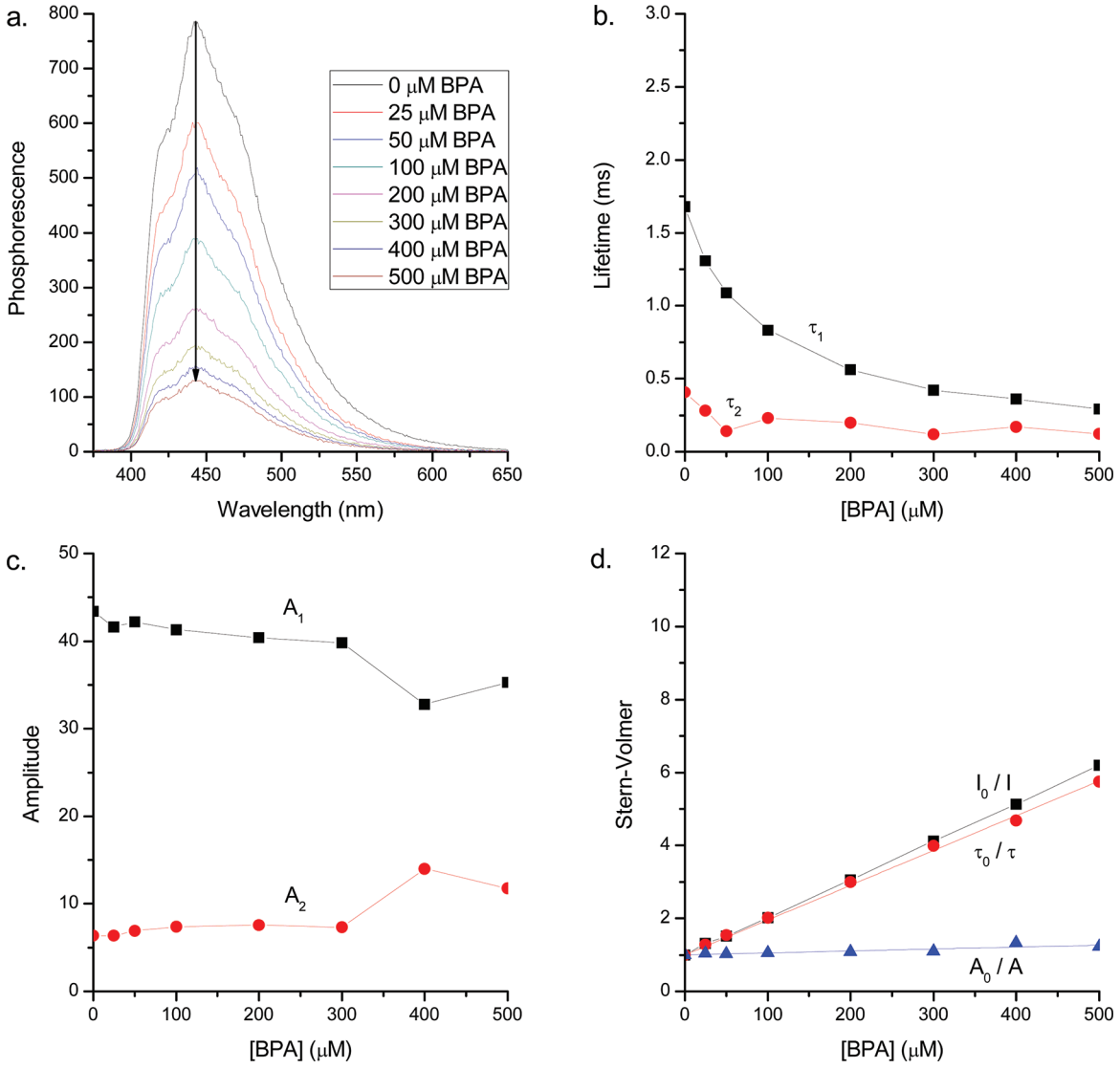

Figure 4. Phosphorescence quenching of 4 μM HSA by 0−500 μM BPA in 20 mM phosphate buffer at pH 7.0. All samples contained 0.2 M KI to enhance the intersystem crossing and 2 mM Na_2SO_3 for deoxygenation. (a) Phosphorescence emission spectra of HSA at different BPA concentrations, (b) phosphorescence lifetimes as a function of BPA concentration, (c) corresponding amplitudes as a function of BPA concentration, and (d) Stern−Volmer plots based on the longest lifetime and its amplitude. τ_1 is the longest HSA lifetime with its amplitude A_1, τ_2 is the shortest HSA lifetime with its amplitude A_2, and I_0, τ_0, and A_0 are the intensity, the longest lifetime, and its amplitude in absence of BPA.

According to this interpretation, the overall static HSA fluorescence spectrum is dominated by conformation I, in which the tryptophan is most exposed to quenching: its DAS does not only show the longest lifetime but also the highest relative amplitude.

Time-resolved fluorescence quenching by BPA was studied over the concentration range from 0.10 to 1.63 mM. The DAS at the highest BPA concentration are depicted in Figures 2b and 3b. Interestingly, the tryptophan fluorescence lifetimes are only little influenced by BPA addition: the longest lifetime is reduced from 7.2 to 6.9 ns (4%) at pH 7.2 and from 6.7 to 5.8 ns (15%) at pH 9.0. In other words, dynamic quenching of fluorescence plays only a negligible role at the BPA concentrations dealt with in this study. The DAS spectra in Figures 2 and 3 show mostly a decrease in amplitude of the long lifetime component. Therefore, the main cause of fluorescence quenching is the static quenching of tryptophan fluorescence in conformer I, while the contributions of conformers II and III are much less affected. This agrees with the hypothesis that multiple conformations with different tryptophan accessibilities exist and supports the use of the modified Stern−Volmer equation for the steady-state quenching data. Similar results (not shown) were obtained when the experiments were repeated at λ_{exc} = 288 nm (close to the absorption maximum) instead of 295 nm (red edge), confirming that the observed changes in amplitude are not due to spectral shifts of the Trp absorption band upon binding.

Room temperature phosphorescence measurements require the presence of KI, and in proteins containing several tryptophan residues, iodide is known to quench the fluorescence of only the solvent-exposed tryptophan moieties.[18] Therefore, we determined the effects of adding KI on the fluorescence characteristics of HSA. Figure 2c shows the DAS obtained in absence and presence of 0.2 M KI at pH 7.2; at pH 9.0 the results were similar (not shown). Also in the presence of 0.2 M KI three lifetimes are observed, but they are significantly shortened. At pH 7.2 the longest lifetime decreases from 7.2 to 4.6 ns (36%) and the second one from 2.6 to 1.8 ns (31%).

dx.doi.org/10.1021/jp300055c | J. Phys. Chem. B 2012, 116, 7033−7039

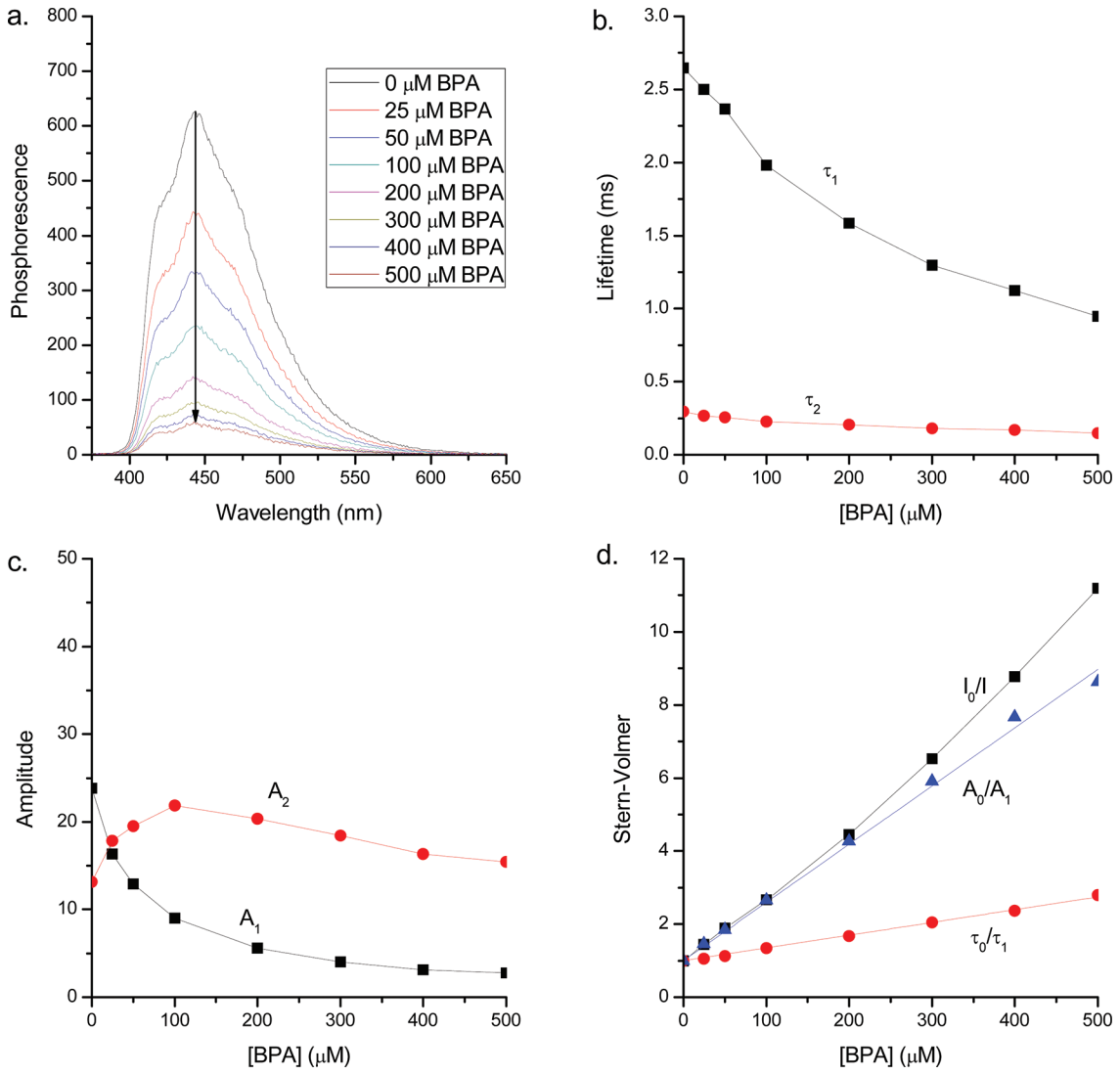

Figure 5. Phosphorescence quenching of 4 μM HSA by 0–500 μM BPA in 20 mM borate buffer at pH 9.0. All samples contained 0.2 M KI to enhance the intersystem crossing and 2 mM Na_2SO_3 for deoxygenation. (a) Phosphorescence emission spectra of HSA at different BPA concentrations, (b) phosphorescence lifetimes as a function of BPA concentration, (c) corresponding amplitudes as a function of BPA concentration, and (d) Stern–Volmer plots based on the longest lifetime and its amplitude. τ_1 is the longest HSA lifetime with its amplitude A_1, τ_2 is the shortest HSA lifetime with its amplitude A_2, and I_0, τ_0, and A_0 are the intensity, the longest lifetime, and its amplitude in the absence of BPA.

Similarly, at pH 9.0 the longest lifetime decreases from 6.7 to 4.5 ns (33%), and the second one from 2.6 to 1.7 ns (35%). Because of the poorer precision, changes in the shortest lifetime of 0.3 ns are not taken into consideration. These lifetime changes indicate that iodide causes a similar degree of dynamic quenching for conformers I and II. Presumably, the heavy atom iodide species—through collisional interaction with tryptophan—causes an enhanced intersystem crossing rate from the first excited singlet state S_1 to the triplet state T_1 and, thus, a reduction in fluorescence lifetime. The bimolecular rate constant for fluorescence quenching by iodide (k^+) can be calculated from the lifetime changes: for conformer I it is about 4×10^8 M^{-1} s^{-1}, and for conformer II it is even somewhat higher at 9×10^8 M^{-1} s^{-1}. As can be seen in Figure 2c, the addition of 0.2 M KI strongly affects the fluorescence intensity of conformer I, which is reduced by a factor of 4. Apparently, for conformer I apart from dynamic quenching also steady-state quenching plays a role: the corresponding equilibrium association constant was calculated to be about $K = 8$ M^{-1}. These results indicate that complex formation of iodide with conformer I influences the tryptophan fluorescence, whereas its association with conformers II and III is of minor importance. The lifetime of this complex can be estimated, since $K = k^+/k^-$ where k^- is the dissociation rate of the complex. Using the values found in the previous paragraph we get $k^- = 5 \times 10^7$ s^{-1}, and thus a lifetime of the complex of about 20 ns. Obviously, this is very short compared to the phosphorescence phenomena to be discussed below.

Phosphorescence. Following the fluorescence experiments, we also studied the static and dynamic effects of BPA on the HSA tryptophan phosphorescence. All samples were chemically deoxygenated to prevent the quenching of phosphorescence by dissolved oxygen. Furthermore, 0.2 M KI was added to all samples to increase the phosphorescence luminescence by accelerating intersystem crossing processes. In addition, we will compare the HSA phosphorescence quenching with that of the free amino acid tryptophan. Since time-resolved phosphorescence measurements must be carried

dx.doi.org/10.1021/jp300055c | J. Phys. Chem. B 2012, 116, 7033–7039

out at a much lower repetition rate than fluorescence experiments (50 Hz vs 4 MHz) and thus show a poorer signal-to-noise ratio, the phosphorescence decays were fitted with a biexponential function. Contrary to the monoexponential decay of free tryptophan (see below), HSA shows at least two phosphorescence lifetimes. The observation of several lifetimes for a protein with a single tryptophan indicates that conformational heterogeneity occurs at the time scale of the phosphorescence emission.[15,16] These cannot be directly compared with the different conformers observed in fluorescence, since different time scales and different quenching mechanisms play a role.

At pH 7 in the absence of BPA, two phosphorescence lifetimes of 1.7 and 0.4 ms are found, with relative amplitudes of 6:1. The fluorescence experiments with KI described above and the larger amplitude of the long-living species indicate that this conformer is relatively accessible to iodide. Figure 4a shows the RTP spectra of 4 μM HSA in the presence of BPA concentrations ranging from 0 to 500 μM. The HSA tryptophan phosphorescence is strongly quenched by BPA, and the corresponding Stern–Volmer plot I_0/I is shown in Figure 4d. In order to evaluate the nature of the quenching mechanism, the phosphorescence lifetimes and associated amplitudes as a function of the BPA concentration are shown in Figure 4b,c, respectively. Upon addition of BPA, the lifetime of the long-living conformer is strongly decreased (Figure 4b), in agreement with a species in which the tryptophan is relatively accessible. The amplitude of this species hardly changes upon adding BPA (Figure 4c); apparently the quenching mechanism at pH 7.0 is mainly dynamic. The Stern–Volmer plot τ_0/τ for the long-lifetime component shows a linear relationship with the BPA concentration, which corresponds with a rate constant of dynamic quenching of $(5.7 \pm 0.2) \times 10^6$ M^{-1} s^{-1} (Figure 4d). The associated minor amplitude change could not be determined very precisely, but the binding constant was estimated from the Stern–Volmer plot A_0/A in Figure 4d as $(5.3 \pm 3.0) \times 10^2$ M^{-1}, reasonably close to the value derived from the static fluorescence experiments described in the previous section ($(2.2 \pm 0.3) \times 10^3$ M^{-1}).

The RTP results at pH 9.0 are quite different from those at neutral pH, as can be seen in Figure 5. Again, two lifetimes are found; the long-living component has a longer lifetime (2.7 ms) and a lower amplitude than at pH 7.0, whereas the short-living component has a slightly shorter lifetime (0.3 ms) and a distinctly higher amplitude than at pH 7.0. By plotting τ_0/τ for the long lifetime component as a function of the BPA concentration (Figure 5d) a linear curve is obtained with a dynamic quenching constant of $(1.3 \pm 0.1) \times 10^6$ M^{-1} s^{-1}, which is 4 to 5 times smaller than at pH 7.0. In a separate set of experiments, we studied the quenching effect of BPA on the phosphorescence of tryptophan free in solution (deoxygenated, in the presence of 0.2 M KI). Both at pH = 7.0 and 9.0, dynamic quenching rates of about 1×10^9 M^{-1} s^{-1} were obtained (data not shown). The rate constants of dynamic quenching for HSA are 2–3 orders of magnitude lower than those for free tryptophan. This indicates that fewer than 1 out of 100 collisions between HSA (long living species) and BPA leads to an effective collision with the tryptophan moiety. In contrast to the results obtained under neutral conditions, at pH 9.0 the phosphorescence of the long-living conformer undergoes not only dynamic quenching but also significant static quenching. From the Stern–Volmer plot A_0/A based on the amplitude of the long-living conformer (Figure 5d), the association constant was calculated to be $(1.6 \pm 0.1) \times 10^4$ M^{-1}. Again, this value is quite close to that found with the static fluorescence quenching experiments described above ($(9.1 \pm 2.2) \times 10^3$ M^{-1}) and confirms the stronger binding of BPA to HSA at higher pH.

CONCLUSIONS

Despite the fact that HSA is a single tryptophan protein, modeling of steady state tryptophan fluorescence quenching of HSA by BPA required the use of the modified Stern–Volmer equation, indicating the existence of an inaccessible fraction of fluorophores. This could be explained by recording the fluorescence decay associated spectra of HSA. Three fluorescence lifetimes associated with different emission spectra were found, which indicates the presence of three conformers of HSA: I, II, and III. Upon addition of BPA, mainly conformer I is amenable to static quenching, whereas complex formation with the tryptophans in conformers II and III plays a negligible role. Apparently, BPA forms a nonfluorescent complex with the exposed tryptophan in conformer I.

In our fluorescence experiments, static quenching by BPA dominates, since at the BPA concentrations applied possible dynamic quenching processes would be too slow to be effective at the nanosecond time scale. At the millimolar quencher level, bimolecular reaction rates as high as 10^{10} M^{-1} s^{-1} would be needed for substantial dynamic fluorescence quenching to occur, whereas in phosphorescence the rate constants required for dynamic quenching are some four decades lower.

Applying the modified Stern–Volmer equation to the fluorescence quenching data, an association constant of $(2.2 \pm 0.3) \times 10^3$ M^{-1} was derived, which agrees very well with the value reported by Martinez-Gomez et al.: $(1.8 \pm 0.3) \times 10^3$ M^{-1}.[4] It should be realized that the latter value refers to the overall BPA–HSA binding, whereas the association constants derived from the Stern–Volmer plots refer only to a binding mode that affects the fluorescence quantum yield. Apparently, in the case of BPA other binding modes or other binding sites do not play a major role. Both the fluorescence and the phosphorescence quenching experiments showed a much stronger binding at higher pH, presumably related to the deprotonated (less polar) state of the alkylamino chain.

Since phosphorescence emission mostly comes from the tryptophan moiety in conformer I interacting with iodide, the HSA conformation with exposed tryptophan dominates the steady state RTP spectra. From the time-resolved RTP spectra not only the binding constants but additionally the biomolecular rate constants of quenching can be derived. These rate constants, $(5.7 \pm 0.2) \times 10^6$ M^{-1} s^{-1} at pH 7.0 and $(1.3 \pm 0.1) \times 10^6$ M^{-1} s^{-1} at pH 9.0, are respectively 100 and 600 times lower than the phosphorescence quenching rate constants determined for free L-Trp. These differences can be attributed to the spatial structure of HSA: in HSA the tryptophan moiety is much less accessible than the free amino acid in solution. The lower dynamic phosphorescence quenching rate and the higher static phosphorescence quenching rate at pH 9 are most probably related to the stronger binding of deprotonated BPA and indicate that a neutral alkylamino side chain is important for binding. The results obtained illustrate that time-resolved fluorescence and phosphorescence spectroscopy are appropriate tools to study HSA–ligand interactions, at two complementary time scales. Apart from site-specific binding constants, also the kinetic versus static nature of binding could be determined.

dx.doi.org/10.1021/jp300055c | J. Phys. Chem. B 2012, 116, 7033–7039

AUTHOR INFORMATION

Corresponding Author

*E-mail g.vander.zwan@vu.nl; tel +31 20 5987635; fax +31 20 5987543.

Author Contributions

†Both authors contributed equally

Notes

The authors declare no competing financial interest.

ACKNOWLEDGMENTS

The authors thank Arjan Wiskerke and Joost Buijs for technical assistance. Financial support was provided by the EU Marie Curie Action program (Grant MEST-CT-2004-008048) to S.T. and by The Netherlands Organisation for Scientific Research (NWO-CW; ECHO Grant No. 700.55.014) to I.L.

REFERENCES

(1) Varshney, A.; Sen, P.; Ahmad, E.; Rehan, M.; Subbarao, N.; Khan, R. H. *Chirality* **2010**, *22*, 77−87.
(2) Dockal, M.; Carter, D. C.; Ruker, F. *J. Biol. Chem.* **1999**, *274*, 29303−29310.
(3) Sulkowska, A. *J. Mol. Struct.* **2002**, *614*, 227−232.
(4) Martinez-Gomez, M. A.; Carril-Aviles, M. M.; Sagrado, S.; Villanueva-Camanas, R. M.; Medina-Hernandez, M. J. *J. Chromatogr. A* **2007**, *1147*, 261−269.
(5) Chadborn, N.; Bryant, J.; Bain, A. J.; O'Shea, P. *Biophys. J.* **1999**, *76*, 2198−2207.
(6) Yoo, M. J.; Schiel, J. E.; Hage, D. S. *J. Chromatogr. B* **2010**, *878*, 1707−1713.
(7) Martinez-Gomez, M. A.; Sagrado, S.; Villanueva-Camanas, R. M.; Medina-Hernandez, M. J. *Electrophoresis* **2006**, *27*, 3410−3419.
(8) Sudlow, G.; Birkett, D. J.; Wade, D. N. *Clin. Exp. Pharmacol. Physiol.* **1975**, *2*, 129−140.
(9) Lakowicz, J. R. *Principles of Fluorescence Spectroscopy*; Springer Verlag: Berlin and Heidelberg, Germany, 2006.
(10) Calhoun, D. B.; Vanderkooi, J. M.; Englander, S. W. *Biochemistry* **1983**, *22*, 1533−1539.
(11) Eftink, M. R.; Selvidge, L. A. *Biochemistry* **1982**, *21*, 117−125.
(12) Gonzalez-Jimenez, J.; Frutos, G.; Cayre, I.; Cortijo, M. *Biochimie* **1991**, *73*, 551−556.
(13) Saviotti, M. L.; Galley, W. C. *Proc. Natl. Acad. Sci. U.S.A.* **1974**, *71*, 4154−4158.
(14) Wei, Y.; Dong, C.; Liu, D.; Shuang, S.; Huie, C. W. *Biomacromolecules* **2007**, *8*, 761−764.
(15) Cioni, P.; Gabellieri, M.; Gonnelli, M.; Strambini, G. B. *Biophys. Chem.* **1994**, *52*, 25−34.
(16) Schlyer, B. D.; Schauerte, J. A.; Steel, D. G.; Gafni, A. *Biophys. J.* **1994**, *67*, 1192−1202.
(17) Telepchak, M. J.; Chaney, G.; August, T. F. *Forensic and clinical applications of solid phase extraction*; Humana Press Inc.: 2004.
(18) Eftink, M. R.; Ghiron, C. A. *Anal. Biochem.* **1981**, *114*, 199−227.